Biological and Environmental Phenomena at the Interface

Influence of the SPR Experimental Conditions on the G-Quadruplex DNA Recognition by Porphyrin Derivatives

Enora Prado, Laureen Bonnat, Hugues Bonnet, Thomas Lavergne, Angeline Van Der Heyden, Genevieve Pratviel, Jerome Dejeu, and Eric Defrancq

Langmuir, **Just Accepted Manuscript** • DOI: 10.1021/acs.langmuir.8b02942 • Publication Date (Web): 07 Oct 2018

Influence of the SPR Experimental Conditions on the G-Quadruplex DNA Recognition by Porphyrin Derivatives

E. Prado,[1] L. Bonnat,[1] H. Bonnet,[1] T. Lavergne,[1] A. Van Der Heyden,[1] G. Pratviel,[2,3] J. Dejeu,[1] E. Defrancq[1]*

1. Univ. Grenoble Alpes, CNRS, DCM, 38000 Grenoble, France

2. CNRS, Laboratoire de Chimie de Coordination, 205 route de Narbonne, BP44099, F-31077 Toulouse Cedex 4, France

3. Université de Toulouse, UPS, INPT, Toulouse, France

KEYWORDS: SPR, G-quadruplex, G4-binding ligands, porphyrin, recognition, surface functionalization, oligonucleotide conjugates

ABSTRACT

Surface plasmon resonance (SPR) is a powerful technique to study the interactions of ligands with analytes and therefore a number of biosensor surfaces and injection methods have been developed so far. However, many experimental parameters can affect the interactions and consequently the affinity measurements. In particular the interactions of positively charged analytes (often used for anionic nucleic acids targets) can be influenced by the sensing surfaces (*e.g.* negatively charged) leading to significant non-specific interactions as well as regeneration problems. The aim of the present work is to investigate the effect of different parameters including ionic strength, SPR biosensor (*i.e.* nature of the surfaces) and the injection method on the recognition of porphyrin G-quadruplex ligands. We demonstrate that the injection method does not influence the affinity whereas the ionic strength and the nature of the surface impact the recognition properties of the porphyrin for the G-quadruplex DNA. We also found that self-assembled monolayer (SAM) coating surface presents many advantages in comparison with carboxymethylated dextran surface for SPR studies of G-quadruplex DNA/ligands interactions: *i)* the electrostatic interaction with charged analytes is less important, *ii)* its structure/composition is less sensitive to the ionic concentration and less prone to unspecific adsorption, *iii)* it is easily home-made and, *iv)* the cost is approximately 10 times cheaper.

Introduction

The surface plasmon resonance is an optical, label-free technique widely used to study the interactions of ligands (including proteins, nucleic acids, sugars and small molecules) with analytes. The ligand is immobilized on the surface while the analyte is injected close to the surface *via* a micro-fluidic system. The analyte recognition by the ligand induces a small change

in the refractive index at the surface/solution interface, which can be quantified with high precision. This technique thus allows the direct detection of mass (concentration) variation without labeling of the analyte. The variation of the refractive index *versus* time (sensorgram) reflects the kinetic and the equilibrium of the interactions. The sensorgrams fitting provide the association and dissociation kinetic constants and the responses obtained at the steady state (R_{eq}) afford the equilibrium dissociation constant. The SPR technique displays a number of advantages including: *(i)* no need for special radioactive or fluorescent labeling of the molecules, *(ii)* time efficiency, *(iii)* use of very low quantity of materials, *(iv)* high sensitivity, and *(v)* access to a variety of commercial surface sensors and the possibility to assemble home-made sensors bearing specific chemical functionalities.[1] However, the diversity of sensing surfaces and the variations of experimental conditions represent serious hurdles for the accurate comparison of results with ones previously published. Few studies investigating the influence of those parameters on recognition processes during SPR measurements have been reported. Cochran *et al*.[2] have found that the affinity values of various ligands for heparin binding proteins obtained with different sensor chips (CM5 and CM4 sensor chips coated with a dextran matrix of different thickness or C1 sensor chips without the dextran matrix) are similar. On the other hand, Drake *et al*.[3] have shown the influence of the dextran matrix (CM5, CM4 and C1 sensors) on the interaction between the ectodomain of the antigen (Ag) and immunoglobulin G1 (IgG1). The dextran matrix exhibits carboxylic acid functions that are negatively charge above pH about 3.5.[4] When the dextran matrix thickness decreases (*i.e.* thereby decreasing the amount of negative charges on the biosensor surface), the affinity, the kinetic and association constants increase (up to a factor of 5) reaching the ones measured in solution. These results could be explained by the effects of the negatively charged carboxyl groups of the dextran, which can *(i)* interact with the

IgG1 antibody and thus sterically hinder the formation of the Ag/IgG1 complex and/or *(ii)* impede the complexation of the IgG1 with Ag due to repulsive interactions with the negatively charged Ag. Fong *et al.* [5] also reported the effects of dextran matrix on the binding kinetics measurements, and attributed them to steric hindrance and to mass transport perturbation. Nevertheless, the dextran matrix has been the most popular sensor surface for SPR experiments with all type of biomolecules (proteins, nucleic acids, glycosides, ...) regardless of the charge of the analytes. Yet, in the context of DNA recognition and in particular with the study of G-quadruplex (G4) binding ligands, the effects of the nature of SPR surfaces could be dramatic.

G4 secondary structures are formed by G-rich DNA sequences and are now considered biologically relevant,[6-9] playing a predominant role in the regulation of many fundamental cellular processes. In particular, the G4 formation at the end of chromosomes (telomeres) and within the promoter region of oncogenes has been found worthy of acute attention as those structures are now considered as novel anticancer drug targets. Indeed, several studies have shown that the inhibition of the telomerase activity (which is overexpressed in cancer cells) and transcriptional repression of oncogenes could be achieved using G4 stabilizing binding ligands.[10] G-quadruplex DNA architecture is a four-stranded structure of stacked guanine tetrads formed by the coplanar arrangement of four guanines, and held together by Hoogsteen bonds. Most of the ligands developed so far are composed of an aromatic part, which can stack over the terminal tetrads, and side chains bearing positive charges for improving the interactions with the phosphodiester DNA backbone as well as for increasing water solubility.[11-22] (references 20-22 added) To investigate the interactions of those ligands with G-quadruplex nucleic acids a number of methods have been developed including FRET-melting, UV-visible spectrophotometry, circular dichroism, NMR and SPR.[23-24] It should be noted that the interaction studies performed

in solution show some limitations due to problems of solubility and aggregation of the G4 binding ligands under the ionic strength conditions required for the stabilization of G-quadruplex DNA.

As aforementioned, a significant number of G4-binding ligands possess positive charges that might be able to interact with the carboxyl group of the dextran present on CM5 or on Streptavidin-grafted CM5 (CM5-SA) sensors during SPR analyses. To limit such interactions, the majority of the analyses were performed with an elevated ionic strength (more than 150 mM of salt) and usually with classical titration (multi cycle kinetic, MCK) [20-22, 25-31](references 25-27 and 31 added)

To the best of our knowledge, the influence of the ionic strength on SPR study of the interactions between G4 and their targeting ligands has not been reported. Such study would be of particular interest since large salt concentrations are usually required to ensure the formation of G4 structures through stabilization of the G-tetrad stacks.

In the past few years, our group has developed an approach termed TASQ (Template Assembled Synthetic G-quadruplex) to constrain, using a cyclopeptide scaffold, G-rich sequences to fold into a single topology with high thermodynamic stability even in the presence of weak ionic strength conditions.[28] By using such G4-forming bioconjugates, we have investigated the interactions of various families of ligands with different G4 structures including parallel DNA and RNA and antiparallel DNA sequences derived from human telomeric sequences and from the promoter region of the HIV-1 long terminal repeat (LTR).[29, 32-33] In our initial report,[29] the injection method (MCK) was optimized using a CM5-SA sensor chip and a running buffer with 350 mM salt. These conditions were experimented with the porphyrin TMPyP4, salophen derivatives and quinacridine MMQ1 and MMQ3.[28] Unfortunately, these conditions were not

suitable for the study of some other G4-binding ligands (as the second generation porphyrin)[31-33] (reference 31-33 added). 30This was notably due to the low solubility of the molecules, the poor regeneration of the surface and/or the occurrence of unspecific interaction of those molecules with the dextran matrix. With the objective to overcome these drawbacks observed with some metal porphyrins ligands, we explore herein the optimization of the injection method, the influence of the surface and the ionic strength of the buffer.

To circumvent problematic regeneration steps, Single Cycle Kinetic method, named SCK method, was used. This method, developed by Karlsson *et al.,* consists in sequential injections of the analyte at increasing concentrations without regeneration steps between each injection.[34-35] To avoid unspecific interactions with 3D dextran matrix, 2D self-assembled monolayers on gold surfaces were also investigated. It is noteworthy that the use of home-made functionalized gold surfaces drastically reduced the cost of experiments (~ 10 times less expensive). These two above-listed modifications have been recently implemented as reported by Bonnat *et al.* for new constrained RNA and HIV quadruplex topologies.[36-37] Furthermore other experimental parameters were varied along the different studies *i.e.* buffer composition, ionic strength to ensure G4 proper folding and/or the solubility of the G4-binding ligands.

To the best of our knowledge, the thorough comparison of the influence of those parameters for SPR analysis has not been described with G-quadruplexes. In the present study, we report on the SPR comparative analysis of G4 binding-ligands interactions by investigating the influence of the buffer ionic strength, the nature of SPR sensor and the injection method. For this study, a porphyrin model (*meso*-tetrakis(4-*N*-methylpyridiniumyl) porphyrin (TMPyP4)) and its metalated Co-$TMPy_2PP$ analog have been selected and the interactions with G4-forming DNA conjugates **1** and **2** have been studied (Figure 1). One of a major mode of TMPyP4 binding with

G-quadruplex DNA is π–π stacking interactions with the external G-quartet.[38] Electrostatic interactions between the four positive pyridiniumyl substituents and the negatively charged phosphate groups of DNA also contribute to increase the binding affinity.[38-39]

Materials and methods

Ligands and analytes preparations

Biomolecular systems **1** and **2** containing DNA sequences derived from the telomeric region of human DNA and which can fold into G-quadruplex were prepared as previously reported.[29] Briefly the systems are composed of *i)* an intermolecular-like quadruplex **1** formed by the tetrastrand assembly of $d[TTAGGGT]_4$, and *ii)* an intramolecular-like quadruplex **2** formed by the sequence $d(GGG(TTAGGG)_3TT)$ (Figure 1A). The porphyrins derivatives (Figure 1B) have been prepared according to previously reported procedure.[31, 40-41]

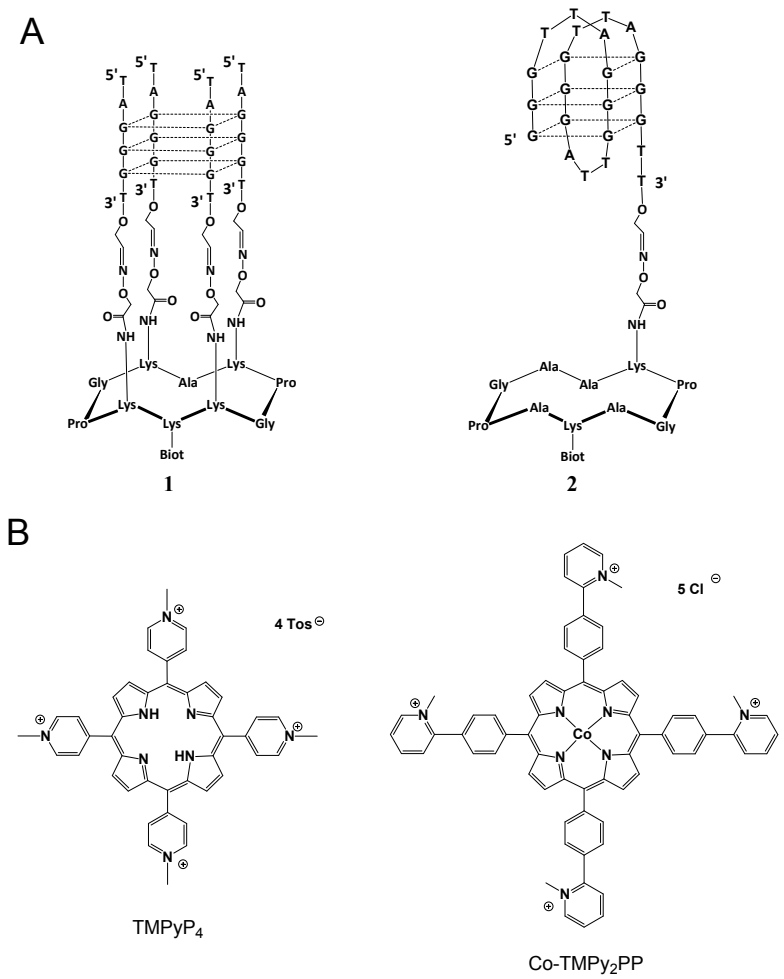

Figure 1. A/ Biomolecular systems containing different DNA structures: intermolecular parallel-stranded quadruplex **1**, and intramolecular folded quadruplex **2**. B/ Structures of G4 binding ligands used in the present study: TMPyP4 and Co-$TMPy_2PP$. Tos stands for tosylate, biot stands for biotin

SPR surface preparation

HS-$(CH_2)_{11}$-EG_4-OH and HS-$(CH_2)_{11}$-EG_6-Biotin were purchased from Prochimia and Sigma Aldrich, respectively. All other chemical products were purchased from Sigma-Aldrich. For simplicity, the terms "thiol-PEG-OH" and "thiol-PEG-Biot" are used to refer to HS-$(CH_2)_{11}$-EG_4-OH and HS-$(CH_2)_{11}$-EG_6-Biotin, respectively. Cleaning procedure included UV-ozone treatment during 10 min followed by rinsing of gold surfaces with MilliQ water then ethanol. Preliminarily cleaned gold surfaces were functionalized according to the following procedure.

Firstly, mixed self-assembled monolayers were formed at room temperature by dipping overnight gold sensors in the mixture of thiols: 90% thiol-PEG-OH and 10% thiol-PEG-Biot (1 mM total thiol concentration in EtOH). After overnight adsorption of thiols, the gold sensors were rinsed with ethanol and dried under nitrogen. Biacore chips were prepared using SAM gold surface and inserted in Biacore T200. Streptavidin (50 ng/mL) were immobilized on SAM surfaces until saturation (response obtained around 2000 R.U.) by injection on four channels (10 µL/min). The different G-quadruplexes were immobilized on streptavidin-coated SAM (SAM-SA) surfaces to obtain a response around 300 R.U. (surfaces saturation). A second surface were prepared using CM5-SA sensor chip (streptavidin-coated surfaces) purchased from BIAcore (GE Healthcare). The different G4-oligonucleotides were immobilized on streptavidin-coated surfaces (CM5-SA sensor chip) to obtain a response around 500 R.U.

SPR analysis

SPR measurements were performed on a BIAcore T200 (GE Healthcare) operating with BIAcore T200 control and evaluation Softwares. All measurements were performed at 25°C using a running buffer (HEPES-buffered saline), which was prepared using either10 mM HEPES (pH 7.4), 35 mM NaCl, 50 mM KCl, and 0.05% (v/v) surfactant P20 termed RB 85, or 10 mM HEPES (pH 7.4), 150 mM NaCl, 200 mM KCl, and 0.05% (v/v) surfactant P20, termed RB 350. A non-modified channel was used as reference. Binding experiments were conducted at 30 $\mu L.min^{-1}$ by injection of the ligand (TMPyP4 or Co-$TMPy_2PP$) during 400s on the four channels. No regeneration step was required. Curves obtained on the reference surface were subtracted from the curves recorded on the other ones, allowing elimination of refractive index changes due to buffer effects and correction of non-specific interactions. The data were fitted using a heterogeneous ligand model. From the non-linear analysis of the sensorgrams the association rate

constants, k_{on1} and k_{on2}, and the dissociation rate constants, k_{off1} and k_{off2} as well as the theoretical maximal response Rmax1 and Rmax2 for the two interactions were calculated. Finally, the equilibrium dissociation constants were calculated from the binding rate constants as $K_{D1} = k_{off1}/k_{on1}$ and $K_{D2} = k_{off2}/k_{on2}$. We report the thermodynamic dissociation constants that were consistent between independent experiments and for which the theoretical maximum response (R_{max}) is consistent with 1:1 interactions. We chose to not report the parameters for the second interaction that might involve non-stoichiometric binding and/or non-specific interactions (see supporting information). The reported values are the mean of representative independent experiments, and the errors provided are standard deviations from the mean.

Results and discussion

To test the influence of experimental variations on the recognition of G-quadruplexes by TMPyP4, different parameters were investigated. The first one consisted in analyzing the injection method.

Influence of the injection method (MCK versus SCK)

Two series of experiments were performed to study the influence of the injection method: one in multi-cycle kinetic (MCK, sensorgram in Figure 1) and the other in single-cycle kinetic (SCK, semsorgrams in Figure 2) on CM5-SA chip in the presence of the high salt concentration RB 350 (see material and methods). The MCK method consists in the repetition of the following steps for each analyte concentration: baseline, association, dissociation, regeneration (if no complete dissociation) whereas for the SCK method, the five analyte concentrations are successively injected without regeneration steps even if the dissociation is not complete. With the SCK method, the dissociation kinetic parameter is determined after the last concentration *i.e.* at the

end of the experiment. The concentration range of TMPyP4 analyte was 50 nM to 2000 nM (Figures 1 and 2).

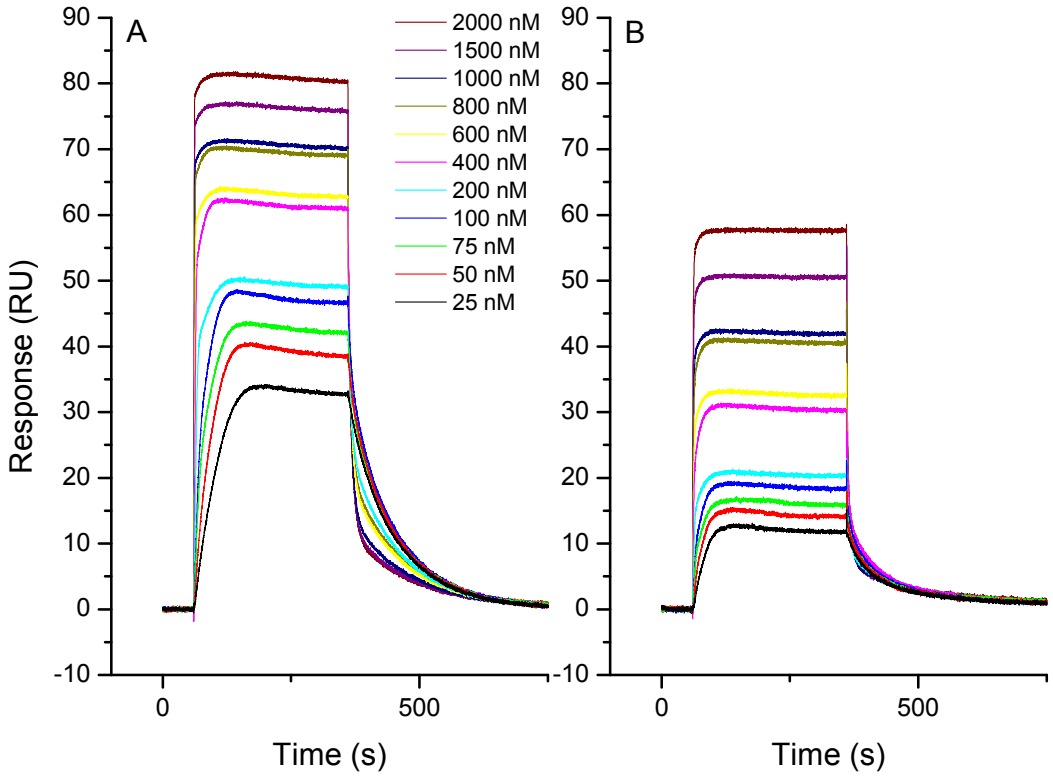

Figure 1. Multi Cycle Kinetic titration analysis realized on CM5-SA sensor chips using RB 350, for the TMPyP4 interaction with A. the intermolecular-like quadruplex **1**, and B. the intramolecular-like quadruplex **2**. The interaction of TMPyP4 with different DNA structures was tested at concentrations of 25, 50, 100, 200, 400, 600, 800, 1000, 1500 and 2000 nM. Sensorgrams correspond to double substracted data (blank and reference subtraction).

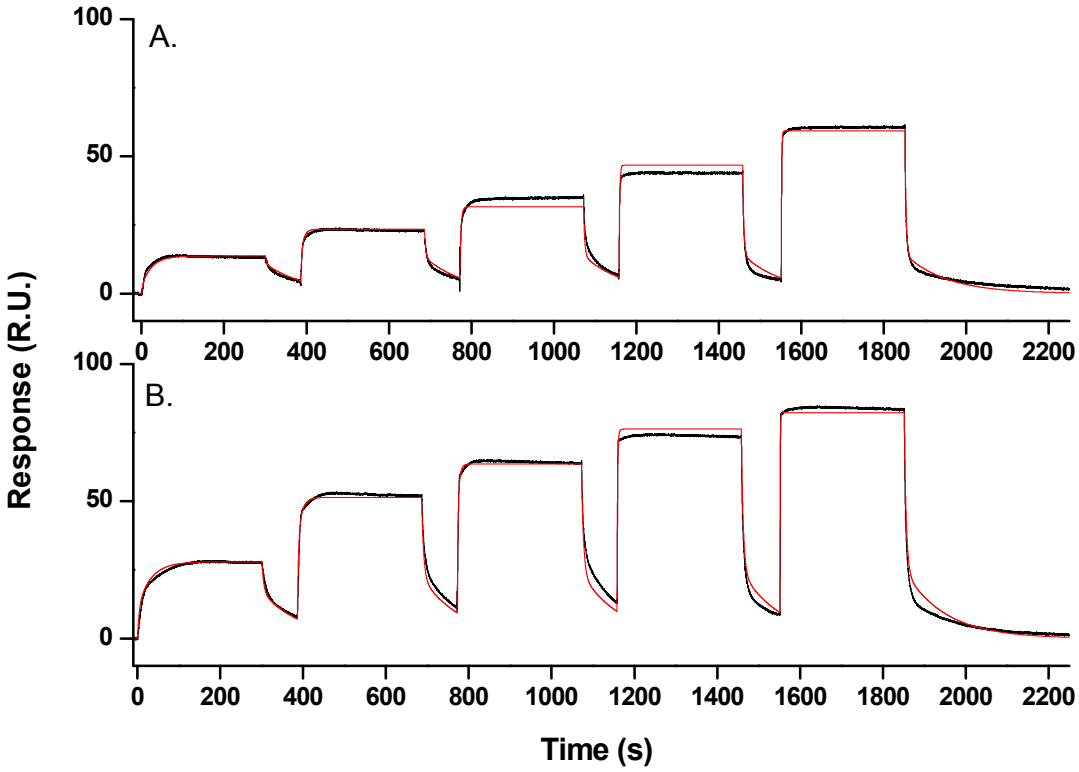

Figure 2. Single Cycle Kinetic titration analysis realized on CM5-SA sensor chips using RB 350, for the TMPyP4 interaction with A. the intermolecular-like quadruplex, B. the intramolecular-like quadruplex. The interaction of TMPyP4 with different DNA structures was tested at concentrations of 50 nM, 200, 500, 1000 and 2000 nM. Sensorgrams corresponded to double substracted data (blank and reference subtraction). Experimental data was plotted in black and fitted curves in red.

Surface	Buffer	Injection method	*Intermolecular quadruplex **1***			*Intramolecular quadruplex **2***		
			k_{on} ($M^{-1}s^{-1}$)	k_{off} (s^{-1})	K_D (nM)	k_{on} ($M^{-1}s^{-1}$)	k_{off} (s^{-1})	K_D (nM)
CM5-SA	RB 350	MCK	$8.9x10^5$	0.12	134±2	$1.9x10^6$	0.76	394±3
		SCK	$8.4x10^5$	0.22	259±4	$3.8x10^5$	0.18	472±40
	RB 85	MCK	$1.7x10^5$	0.14	868±6	$1.9x10^5$	0.18	887±10
		SCK	$3.1x10^5$	0.27	892±33	$9.3x10^4$	0.08	849±22
SAM-SA	RB 350	SCK	$4.0x10^6$	0.15	37±4	$9.0x10^6$	0.53	61±5
	RB 85	SCK	$6.0x10^6$	0.22	37±2	$5.0x10^6$	0.29	58±16

Table 1. Kinetic parameters of TMPyP4 interactions with quadruplex DNA structures **1** and **2** on CM5-SA and SAM-SA chips. Analyses were carried out on chips using two injections methods (Single cycle kinetic, SCK and multicycle kinetic, MCK) and for two ionic concentrations (RB 350 and RB 85). k_{on}: association rate, k_{off}: dissociation rate, and K_D: equilibrium dissociation constant deduced from the kinetic rate constants.

The values of equilibrium dissociation constants (K_D) of TMPyP4 interactions with quadruplex DNA structures **1** and **2** were 134 nM and 394 nM, respectively in RB 350 (Table 1). These values are in agreement with previously reported data[42-45] and thus demonstrate that TMPyP4 can be used as a model system to study the influence of the experimental parameters on porphyrin/G4-DNA interactions. In Table 1, it can be observed that the K_D values obtained for both injection methods are concordant at a given ionic strength. This result confirms that the SCK method is a viable alternative to reduce the experimental time and paves the way to the characterization of problematic G4-binding ligands for which no regeneration step can be achieved.[46]

Influence of ionic strength (RB 350 versus RB 85)

To evaluate the influence of the ionic strength on the measurement of the affinity we compared the use of RB 350 with a lower ionic strength buffer (RB 85). In addition to this effect on charge

neutralization, buffer ionic strength may also affect the porphyrin solubility. Indeed, whereas porphyrins endowed with charged substituents are readily soluble in water they may undergo self-stacking, which is further promoted by increasing ionic strength.[47-51] Induced self-stacking as the result of binding to DNA may also occur. It is also noteworthy that under low ionic strength (RB 85) template-assembled G4 **1** and **2** still form stable G4 fold. However, the topologies of intramolecular like G-quadruplex **2** being dependent of the ionic nature and proportion, K^+/Na^+ ratio was kept constant.[52] The effect of ionic concentration on equilibrium dissociation constants was studied on CM5-SA sensors chips with MCK (Figure SI-2) and SCK (Figure SI-3) methods (Table 1).

Equilibrium dissociation constants of each TMPyP4/DNA complexes were found once again similar for both injection methods, confirming the validity of SCK method to characterize kinetic and thermodynamic parameters of G-quadruplex interactions. However, the TMPyP4 affinity, for both G-quadruplexes **1** and **2**, diminished when the buffer concentration decreased. These results are concordant with the study from Freyer *et al.*,[53] who have shown that the affinity of TMPyP4 for G-quadruplex DNA slightly decreases when the KCl concentration increases from 20 mM to 200 mM. This study also demonstrated, through computaional modeling and ITC investigations, that the electrostatic contribution to TMPyP4/G4 DNA affinity was small.

Our results could be explained by the interaction of TMPyP4 with dextran matrix through unspecific interaction similar to that previously reported for other biorecognition studies.[3, 5] Indeed, when the ionic strength decreases, the charge screening of the dextran matrix is less efficient and consequently the electrostatic interactions between the four positive charges of the TMPyP4 analyte and the negative charges of the dextran are favored. This hypothesis is

strengthened by the results obtained with SAM-SA sensors for which we observed no difference in affinity when lowering the buffer concentration *(vide infra)*.

Influence of the surface (CM5-SA versus SAM-SA)

The research of the most appropriate surface is a key point to allow for a reliable analysis of the kinetic parameter of the interactions. As an alternative to dextran, flat surfaces can be coated by adequately functionalized self-assembled monolayers. Many approaches exist to form functional SAMs onto thin gold SPR films.[54] The most widely used approach is based on thiolated organic compounds, which spontaneously form self-assembled monolayers on gold surfaces. Polymeric layers (*i.e.* dextran for CM5-SA chip) and self-assembled monolayers (SAM-SA) show significant differences.[55] In the two-dimensional structure of SAMs, the ligands are oriented on the surface in the same direction, whereas polymeric layers depict a three-dimensional structure, which triggers a randomized orientation of the ligands (see supporting information Figure SI-1). Furthermore, it is usually harder for the analytes to diffuse through 3D hydrogels than through 2D-SAMs and the kinetics of the interactions can thereby be altered.[56] Despite these differences, several reports show that there is no major difference in binding kinetics between SAMs and dextran hydrogel.[57-58] Yet, SAMs modified surfaces are generally considered better compared to dextran hydrogel for kinetic parameter determination, especially when low amounts of immobilized ligand is required and when the level of non-specific binding has to be kept to a minimum.[59] For SAM, reduction of non-specific binding can be accomplished by including compounds such as polyethylene glycol derivatives for the immobilization steps.[60]

To explore the effect of the surface, we designed SAMs chips with mixed self-assembled monolayers of thiol-PEG-OH and thiol-PEG-Biot (in a ratio of 1 to 9), that allow efficient

surface saturation with biotin moieties. Such PEG SAMs have also been shown to have an excellent stability and good reproducibility, in addition to a decrease of non-specific binding.[61-62] Following the surface saturation by streptavidin, biomolecular systems **1-2** were immobilized through biotin-streptavidin interactions. The surface saturation was achieved around a signal variation of 300 R.U. According to Jung's equation (see supporting information),[63] the G4 quantity on SAM-SA is two time less to that obtained on CM5-SA chips (around 500 R.U.), justified by the different configuration of the surface (see Figure SI-1).

The affinity measurements for TMPyP4 interaction with both G-quadruplexes **1-2** were acquired on these SAM chips in presence of buffer 350 (Figure SI-4) or buffer 85 (Figure SI-5), respectively. The other conditions (*i.e.* concentration range, injection times) were kept identical (Table 1).

Unlike with CM5-SA (Table 1), no ionic effect was observed by using SAM-SA chips: the binding parameters remained similar for TMPyP4 interaction with each G4 in RB 85 or RB 350 (Table 1). By using RB 350, it was observed that K_D values for the interaction between TMPyP4 and both G-quadruplexes **1-2** are lower on SAM-SA than on CM5-SA chips (Table 1). This difference manifests itself in the variation of the kinetic association constant: a significant increase of k_{on} is observed for the interaction of TMPyP4 for both quadruplexes **1** and **2** when using SAM-SA chip (8.4×10^5 $M^{-1}s^{-1}$ *versus* 4.0×10^6 $M^{-1}s^{-1}$ and 3.8×10^5 $M^{-1}s^{-1}$ *versus* 9.0×10^6 $M^{-1}s^{-1}$ for the interaction with **1** and **2**, respectively (Table 1)) whereas the dissociation constant k_{off} remains nearly identical for both surfaces. Such effect on k_{on} has been previously described with protein/protein and antibody/antigen interaction studied on 2D or 3D matrixes.[3, 5] Those results have been explained by an easier access of the analytes to the surface bound ligands. Similar results were obtained for TMPyP4 with RB 85.

Due to self-stacking at high salt concentration, the interaction of the metalated Co-TMPy$_2$PP porphyrin with G4 **1** and **2** was only carried out at low salt concentration (RB 85). K_D values were lower when using SAM-SAs *versus* CM5-SA chip[31-32] and we also observed increase in association rate with SAM-SAs chip (Table 2).

Surface	*Intermolecular quadruplex **1***			*Intramolecular quadruplex **2***		
	k_{on} ($M^{-1}s^{-1}$)	k_{off} (10^{-5} s^{-1})	K_D (nM)	k_{on} ($M^{-1}s^{-1}$)	k_{off} ($10^{-5}s^{-1}$)	K_D (nM)
CM5-SA[a]	$2.2x10^3$	3.8	17.0 ± 0.4	$2.5x10^3$	15.0	60.2 ± 1.9
SAM-SA[b]	$2.8x10^4$	9.5	3.4 ± 0.2	$7.8x10^3$	11.5	15.0 ± 0.2

Table 2. Kinetic parameters of Co-TMPy$_2$PP interactions with G-quadruplex DNA structures **1** and **2**. Analyses were performed on SA and SAM chips with a RB 85 using SCK method. k_{on}: association rate, k_{off}: dissociation rate, and K_D: dissociation equilibrium constant deduced from the kinetic rate constants. [a] K_D value from reference [31], [b] K_D value from reference [32]

For both TMPyP4 and Co-TMPy$_2$PP, the better affinity and faster association rate observed on SAM-SA surfaces could be attributed to a favorable G4 orientation and/or the absence of unspecific electrostatic interactions. Indeed, on SAM-SA sensor, the G-quadruplex recognition motifs are oriented toward the top of the surface layer allowing easy access for the analytes whereas on CM5-SA chip a random orientation occurs within the depth of the dextran matrix with possible steric hindrances. Moreover, on SAM-SA, no charged matrix is present to disturb the interaction as already observed by several researchers using charged analytes.[3, 5] All together, these results show that the homogenous ligand orientation and the absence of charged matrix, offered by SAM-SA chip, significantly facilitate the interactions and allow for the reliable determination of kinetic and thermodynamic parameters.

Conclusion

In this paper, the influence of the experimental conditions (*i.e* ionic strength, nature of the surface, injection method) on SPR analysis of ligand/G-quadruplex DNA interactions was investigated by using TMPyP4 as a model G4-binding ligand. We could demonstrate that the injection method does not influence the value of the kinetic and thermodynamic constants. However, for the two other parameters (*i.e.* ionic strength and nature of the surface), the recognition properties of the porphyrin G4-binding ligands for the G-quadruplex DNA are impacted. The affinities decreased with the ionic strength when using CM5-SA chip (*i.e.* dextran surface), whereas on SAM-SA chip, no variation was observed. This can be explained by the interaction of the cationic G4-binding ligands with the negative charges of the dextran matrix. On the other hand, the affinity was found to be higher on SAM-SA chip due to faster association rate, which could be attributed to a more favorable presentation of the G4 on the 2D surface.

In conclusion, the SAM-SA surface was found to possess advantages over CM5-SA surface for SPR studies of G-quadruplex DNA/ligands interactions. First, SAM-SA chips are insensitive to ionic strength variation and allow easy access to the analytes. Furthermore, the chips could be easily home-made with a cost approximately 10 times lower than that of CM5-SA chips.

ASSOCIATED CONTENT

Supporting Information. All sensorgrams were presented on the Supporting Information. The following files are available free of charge.

AUTHOR INFORMATION

Corresponding Author

Correspondence and requests for materials should be addressed to Jérôme Dejeu: email: jerome.dejeu@univ-grenoble-alpes.fr

Author Contributions

The manuscript was written through contributions of all authors. All authors have given approval to the final version of the manuscript.

ACKNOWLEDGMENT

We are grateful to Agence Nationale pour la Recherche (ANR G4-TopiPro ANR-16-CE11-0006-01 and ANR Quarpdiems ANR-12-BSV8-0008-01), Labex ARCANE (ANR-11-LABX-0003-01). The authors acknowledge support from ICMG FR 2607 for providing synthesis and purification of oligonucleotides and SPR facilities.

Graphical abstract

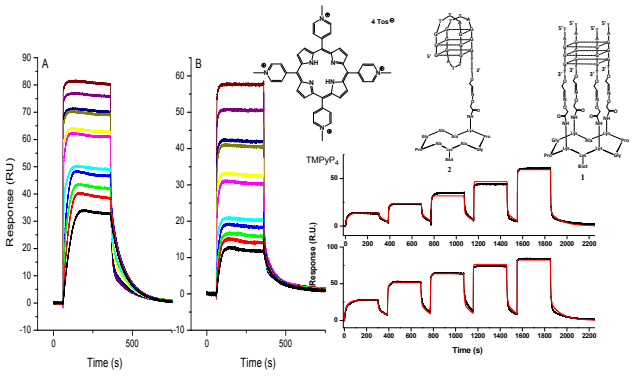

REFERENCES

1. Schasfoort, R. B. M., *Handbook of Surface Plasmon Resonance: Edition 2*. 2017; p 1-524.
2. Cochran, S.; Li, C. P.; Ferro, V., A Surface Plasmon Resonance-Based Solution Affinity Assay for Heparan Sulfate-Binding Proteins. *Glycoconjugate J.* **2009,** *26*, 577-587.

3. Drake, A. W.; Tang, M. L.; Papalia, G. A.; Landes, G.; Haak-Frendscho, M.; Klakamp, S. L., Biacore Surface Matrix Effects on the Binding Kinetics and Affinity of an Antigen/Antibody Complex. *Anal. Biochem.* **2012,** *429*, 58-69.
4. *Biacore Assay Handbook 29-0194-00 Edition AA 19*.
5. Fong, C.-C.; Wong, M.-S.; Fong, W.-F.; Yang, M., Effect of Hydrogel Matrix on Binding Kinetics of Protein–Protein Interactions on Sensor Surface. *Anal. Chim. Acta* **2002,** *456*, 201-208.
6. Rodriguez, R.; Miller, K. M.; Forment, J. V.; Bradshaw, C. R.; Nikan, M.; Britton, S.; Oelschlaegel, T.; Xhemalce, B.; Balasubramanian, S.; Jackson, S. P., Small-Molecule-Induced DNA Damage Identifies Alternative DNA Structures in Human Genes. *Nat. Chem. Biol.* **2012,** *8*, 301-310.
7. Biffi, G.; Tannahill, D.; McCafferty, J.; Balasubramanian, S., Quantitative Visualization of DNA G-Quadruplex Structures in Human Cells. *Nat. Chem.* **2013,** *5*, 182-186.
8. Biffi, G.; Di Antonio, M.; Tannahill, D.; Balasubramanian, S., Visualization and Selective Chemical Targeting of RNA G-Quadruplex Structures in the Cytoplasm of Human Cells. *Nat. Chem.* **2014,** *6*, 75-80.
9. Laguerre, A.; Hukezalie, K.; Winckler, P.; Katranji, F.; Chanteloup, G.; Pirrotta, M.; Perrier-Cornet, J. M.; Wong, J. M. Y.; Monchaud, D., Visualization of RNA-Quadruplexes in Live Cells. *J. Am. Chem. Soc.* **2015,** *137*, 8521-8525.
10. Muller, S.; Rodriguez, R., G-quadruplex Interacting Small Molecules and Drugs: from Bench toward Bedside. *Expert Rev. Clin. Pharmacol.* **2014,** *7*, 663-679.
11. Nielsen, N. C.; Ulven, T., Macrocyclic G-Quadruplex Ligands. *Curr. Med. Chem.* **2010,** *17*, 3438-3448.
12. Neidle, S., Quadruplex Nucleic Acids as Novel Therapeutic Targets. *J. Med. Chem.* **2016,** *59*, 5987-6011.
13. Neidle, S., Quadruplex Nucleic Acids as Targets for Anticancer Therapeutics. *Nat. Rev. Chem.* **2017,** *1*.
14. Zhang, S. L.; Wu, Y. L.; Zhang, W., G-Quadruplex Structures and Their Interaction Diversity with Ligands. *Chemmedchem* **2014,** *9*, 899-911.
15. Maji, B.; Bhattacharya, S., Advances in the Molecular Design of Potential Anticancer Agents Via Targeting of Human Telomeric DNA. *Chem. Commun.* **2014,** *50*, 6422-6438.
16. Piraux, G.; Bar, L.; Abraham, M.; Lavergne, T.; Jamet, H.; Dejeu, J.; Marcelis, L.; Defrancq, E.; Elias, B., New Ruthenium-Based Probes for Selective G-Quadruplex Targeting. *Chem. Eur. J.* **2017,** *23*, 11872-11880.
17. Zhang, S. Y.; Wu, Q.; Zhang, H.; Wang, Q.; Wang, X. C.; Mei, W. J.; Wu, X. H.; Zheng, W. J., Microwave-Assisted Synthesis of Ruthenium(II) Complexes With Alkynes as Potential Inhibitor by Selectively Recognizing c-myc G-Quadruplex DNA. *J. Inorg. Biochem.* **2017,** *176*, 113-122.
18. Yang, D. Z.; Okamoto, K., Structural Insights into G-quadruplexes: Towards New Anticancer Drugs. *Future Med. Chem.* **2010,** *2*, 619-646.
19. Łęczkowska, A.; Gonzalez-Garcia, J.; Perez-Arnaiz, C.; Garcia, B.; White, A. J. P.; Vilar, R., Binding Studies of Metal–Salphen and Metal–Bipyridine Complexes Towards G-Quadruplex DNA. *Chem. Eur. J.* **2018,** *24*, 11785-11794.
20. Dash, J.; Waller, Z. A. E.; Pantoş, G. D.; Balasubramanian, S., Synthesis and Binding Studies of Novel Diethynyl-Pyridine Amides with Genomic Promoter DNA G-Quadruplexes. *Chem. Eur. J.* **2011,** *17*, 4571-4581.

21. Panda, D.; Saha, P.; Das, T.; Dash, J., Target Guided Synthesis Using DNA Nano-Templates for Selectively Assembling a G-Quadruplex Binding c-MYC Inhibitor. *Nature Communications* **2017,** *8*, 16103.
22. Dash, J.; Shirude, P. S.; Hsu, S.-T. D.; Balasubramanian, S., Diarylethynyl Amides That Recognize the Parallel Conformation of Genomic Promoter DNA G-Quadruplexes. *J. Am. Chem. Soc.* **2008,** *130*, 15950-15956.
23. Jaumot, J.; Gargallo, R., Experimental Methods for Studying the Interactions between G-Quadruplex Structures and Ligands. *Curr. Pharm. Des.* **2012,** *18*, 1900-1916.
24. Murat, P.; Singh, Y.; Defrancq, E., Methods for Investigating G-Quadruplex DNA/Ligand Interactions. *Chem. Soc. Rev.* **2011,** *40*, 5293-5307.
25. Toro, M. D.; Gargallo, R.; Eritja, R.; Jaumot, J., Study of the Interaction Between the G-Quadruplex-Forming Thrombin-Binding Aptamer and the Porphyrin 5,10,15,20-tetrakis-(N-methyl-4-pyridyl)-21,23H-Porphyrin Tetratosylate. *Anal. Biochem.* **2008,** *379*, 8-15.
26. Arora, A.; Maiti, S., Effect of Loop Orientation on Quadruplex−TMPyP4 Interaction. *The Journal of Physical Chemistry B* **2008,** *112*, 8151-8159.
27. Gonçalves, D. P. N.; Ladame, S.; Balasubramanian, S.; Sanders, J. K. M., Synthesis and G-Quadruplex Binding Studies of New 4-N-methylpyridinium Porphyrins. *Org. Biomol. Chem.* **2006,** *4*, 3337-3342.
28. Murat, P.; Cressend, D.; Spinelli, N.; Van der Heyden, A.; Labbé, P.; Dumy, P.; Defrancq, E., A Novel Conformationally Constrained Parallel G Quadruplex. *ChemBioChem* **2008,** *9*, 2588-2591.
29. Murat, P.; Bonnet, R.; Van der Heyden, A.; Spinelli, N.; Labbé, P.; Monchaud, D.; Teulade-Fichou, M.-P.; Dumy, P.; Defrancq, E., Template-Assembled Synthetic G-Quadruplex (TASQ): A Useful System for Investigating the Interactions of Ligands with Constrained Quadruplex Topologies. *Chem. Eur. J.* **2010,** *16*, 6106-6114.
30. Lecarme, L.; Prado, E.; De Rache, A.; Nicolau-Travers, M.-L.; Bonnet, R.; Heyden, A. v. D.; Philouze, C.; Gomez, D.; Mergny, J.-L.; Jamet, H.; Defrancq, E.; Jarjayes, O.; Thomas, F., Interaction of Polycationic Ni(II)-Salophen Complexes with G-Quadruplex DNA. *Inorg. Chem.* **2014,** *53*, 12519-12531.
31. Sabater, L.; Fang, P. J.; Chang, C. F.; De Rache, A.; Prado, E.; Dejeu, J.; Garofalo, A.; Lin, J. H.; Mergny, J. L.; Defrancq, E.; Pratviel, G., Cobalt(III) Porphyrin to Target G-Quadruplex DNA. *Dalton Trans.* **2015,** *44*, 3701-3707.
32. Dejeu, J.; Lavergne, T.; Nora, J. D.; Defrancq, E.; Pratviel, G., Binding of Metalloporphyrins to G-Quadruplex DNA: The Role of the Central Metal. *Inorg. Chim. Acta* **2016,** *452*, 98-103.
33. Sabater, L.; Nicolau-Travers, M.-L.; De Rache, A.; Prado, E.; Dejeu, J.; Bombarde, O.; Lacroix, J.; Calsou, P.; Defrancq, E.; Mergny, J.-L.; Gomez, D.; Pratviel, G., The Nickel(II) Complex of Guanidinium Phenyl Porphyrin, a Specific G-Quadruplex Ligand, Targets Telomeres and leads to POT1 Mislocalization in Culture Cells. *J. Biol. Inorg. Chem.* **2015,** *20*, 729-738.
34. Karlsson, R.; Katsamba, P. S.; Nordin, H.; Pol, E.; Myszka, D. G., Analyzing a Kinetic Titration Series using Affinity Biosensors. *Anal. Biochem.* **2006,** *349*, 136-147.
35. Palau, W.; Di Primo, C., Simulated Single-Cycle Kinetics improves the Design of Surface Plasmon Resonance Assays. *Talanta* **2013,** *114*, 211-216.

36. Bonnat, L.; Dejeu, J.; Bonnet, H.; Gennaro, B.; Jarjayes, O.; Thomas, F.; Lavergne, T.; Defrancq, E., Templated Formation of Discrete RNA and DNA:RNA Hybrid G-Quadruplexes and Their Interactions with Targeting Ligands. *Chem. Eur. J.* **2016,** *22*, 3139-3147.
37. Bonnat, L.; Bar, L.; Gennaro, B.; Bonnet, H.; Jarjayes, O.; Thomas, F.; Dejeu, J.; Defrancq, E.; Lavergne, T., Template-Mediated Stabilization of a DNA G-Quadruplex formed in the HIV-1 Promoter and Comparative Binding Studies. *Chem. Eur. J.* **2017,** *23*, 5602-5613.
38. Phan, A. T.; Kuryavyi, V.; Gaw, H. Y.; Patel, D. J., Small-Molecule Interaction with a Five-Guanine-tract G-Quadruplex Structure from the Human MYC Promoter. *Nat. Chem. Biol.* **2005,** *1*, 234-234.
39. Parkinson, G. N.; Ghosh, R.; Neidle, S., Structural Basis for Binding of Porphyrin to Human Telomeres. *Biochemistry* **2007,** *46*, 2390-2397.
40. Han, F. X. G.; Wheelhouse, R. T.; Hurley, L. H., Interactions of TMPyP4 and TMPyP2 with Quadruplex DNA. Structural Basis for the Differential Effects on Telomerase Inhibition. *J. Am. Chem. Soc.* **1999,** *121*, 3561-3570.
41. Romera, C.; Sabater, L.; Garofalo, A.; M. Dixon, I.; Pratviel, G., Interaction of Cationic Nickel and Manganese Porphyrins with the Minor Groove of DNA. *Inorg. Chem.* **2010,** *49*, 8558-8567.
42. Wei, C. Y.; Jia, G. Q.; Yuan, J. L.; Feng, Z. C.; Li, C., A Spectroscopic Study on the Interactions of Porphyrin with G-Quadruplex DNAs. *Biochemistry* **2006,** *45*, 6681-6691.
43. Seenisamy, J.; Bashyam, S.; Gokhale, V.; Vankayalapati, H.; Sun, D.; Siddiqui-Jain, A.; Streiner, N.; Shin-ya, K.; White, E.; Wilson, W. D.; Hurley, L. H., Design and Synthesis of an Expanded Porphyrin that has Selectivity for the c-MYC G-Quadruplex Structure. *J. Am. Chem. Soc.* **2005,** *127*, 2944-2959.
44. Romera, C.; Bombarde, O.; Bonnet, R.; Gomez, D.; Dumy, P.; Calsou, P.; Gwan, J. F.; Lin, J. H.; Defrancq, E.; Pratviel, G., Improvement of Porphyrins for G-Quadruplex DNA Targeting. *Biochimie* **2011,** *93*, 1310-1317.
45. Perez-Arnaiz, C.; Busto, N.; Santolaya, J.; Leal, J. M.; Barone, G.; Garcia, B., Kinetic Evidence for Interaction of TMPyP4 with Two Different G-Quadruplex Conformations of Human Telomeric DNA. *Biochim. Biophys. Acta* **2018,** *1862*, 522-531.
46. During our investigations, we have repeatedly found that some G4-binding ligands were very difficult to remove from their target and tend to accumulate into the micro-fluidic device.
47. Pasternack, R. F., Aggregation Properties of Water-Soluble Porphyrins. *Ann. N.Y. Acad. Sci.* **1973,** *206*, 614-630.
48. Dixon, D. W.; Steullet, V., Dimerization of Tetracationic Porphyrins: Ionic Strength Dependence. *J. Inorg. Biochem.* **1998,** *69*, 25-32.
49. Manono, J.; Marzilli, P. A.; Marzilli, L. G., New Porphyrins Bearing Positively Charged Peripheral Groups Linked by a Sulfonamide Group to meso-Tetraphenylporphyrin: Interactions with Calf Thymus DNA. *Inorg. Chem.* **2009,** *48*, 5636-5647.
50. Fiel, R. J.; Howard, J. C.; Mark, E. H.; Dattagupta, N., Interaction of DNA with a Porphyrin Ligand - Evidence for Intercalation. *Nucleic Acids Res.* **1979,** *6*, 3093-3118.
51. Carvlin, M. J.; Fiel, R. J., Intercalative and Nonintercalative Binding of Large Cationic Porphyrin Ligands to Polynucleotides to Calf Thymus DNA. *Nucleic Acids Res.* **1983,** *11*, 6121-6139.
52. Gray, R. D.; Li, J.; Chaires, J. B., Energetics and Kinetics of a Conformational Switch in G-Quadruplex DNA. *J. Phys. Chem. B* **2009,** *113*, 2676-2683.

53. Freyer, M. W.; Buscaglia, R.; Kaplan, K.; Cashman, D.; Hurley, L. H.; Lewis, E. A., Biophysical Studies of the c-MYC NHE III1 Promoter: Model Quadruplex Interactions With a Cationic Porphyrin. *Biophysical Journal* **2007,** *92*, 2007-2015.
54. Ulman, A., Formation and Structure of Self-Assembled Monolayers. *Chem. Rev.* **1996,** *96*, 1533-1554.
55. Wijaya, E.; Lenaerts, C.; Maricot, S.; Hastanin, J.; Habraken, S.; Vilcot, J. P.; Boukherroub, R.; Szunerits, S., Surface Plasmon Resonance-Based Biosensors: From the Development of Different SPR Structures to Novel Surface Functionalization Strategies. *Curr. Opin. Solid State Mater. Sci.* **2011,** *15*, 208-224.
56. Svitel, J.; Schuck, P., Combined Affinity and Rate Constant Distributions of Ligand Populations from Experimental Surface-Binding Kinetics and Equilibria. *Biophysical Journal* **2004,** *86*, 22A-22A.
57. Lahiri, J.; Isaacs, L.; Tien, J.; Whitesides, G. M., A Strategy for the Generation of Surfaces Presenting Ligands for Studies of Binding Based on an Active Ester as a Common Reactive Intermediate: A Surface Plasmon Resonance Study. *Anal. Chem.* **1999,** *71*, 777-790.
58. Kausaite-Minkstimiene, A.; Ramanaviciene, A.; Kirlyte, J.; Ramanavicius, A., Comparative Study of Random and Oriented Antibody Immobilization Techniques on the Binding Capacity of Immunosensor. *Anal. Chem.* **2010,** *82*, 6401-6408.
59. Kyprianou, D.; Guerreiro, A. R.; Nirschl, M.; Chianella, I.; Subrahmanyam, S.; Turner, A. P. F.; Piletsky, S., The Application of Polythiol Molecules for Protein Immobilisation on Sensor Surfaces. *Biosens. Bioelectron.* **2010,** *25*, 1049-1055.
60. Zareie, H. M.; Boyer, C.; Bulmus, V.; Nateghi, E.; Davis, T. P., Temperature-Responsive Self-Assembled Monolayers of Oligo(ethylene glycol): Control of Biomolecular Recognition. *ACS Nano* **2008,** *2*, 757-765.
61. Nileback, E.; Feuz, L.; Uddenberg, H.; Valiokas, R.; Svedhem, S., Characterization and Application of a Surface Modification Designed for QCM-D Studies of Biotinylated Biomolecules. *Biosens. Bioelectron.* **2011,** *28*, 407-413.
62. Zhang, X. J.; Yadavalli, V. K., Surface Immobilization of DNA Aptamers for Biosensing and Protein Interaction Analysis. *Biosens. Bioelectron.* **2011,** *26*, 3142-3147.
63. Jung, L. S.; Campbell, C. T.; Chinowsky, T. M.; Mar, M. N.; Yee, S. S., Quantitative Interpretation of the Response of Surface Plasmon Resonance Sensors to Adsorbed Films. *Langmuir* **1998,** *14*, 5636-5648.